University of BRISTOL

November 2013

# Seismic Monitoring of Drilling Operations In Balcombe, West Sussex

Dr Anna Horleston
Dr Anna Stork
Dr James Verdon
Dr Alan Baird
Dr James Wookey
Professor Michael Kendall

# EXECUTIVE SUMMARY


- There is a small but finite risk that hydraulic fracturing for shale gas can trigger felt seismic events. DECC have introduced a traffic light scheme, whereby operations will be halted if events above a certain size are triggered.

- In order to meet this requirement, seismic monitoring arrays will be required at future hydraulic fracturing sites. Moreover, baseline monitoring will be required to establish background rates of naturally occurring seismicity, such that any variation induced by hydraulic fracturing can be established.

- Drilling of an exploratory well by Cuadrilla at their Balcombe site has provoked significant public interest in the potential benefits and risks of shale gas development in the UK.

- We deployed a small network of 4 broadband seismometers for 1 month prior to, and for the full duration of, Cuadrilla's Balcombe operations. This array has allowed us to establish background noise levels, and provided some information on detectability thresholds, and background rates of seismicity.

- Numerous sources of seismic noise were identified. In particular, the main London-to-Brighton rail line, which passes alongside the study area, was a major source of noise. The ground motion due to a passing train measured at a distance of 150 m from the rail line is approximately equivalent in amplitude to the ground motion that would be recorded at this location if a magnitude 1.5 earthquake occurred 2 km below the drilling site.

- An automated triggering algorithm was used to search the recorded data for local seismicity. 134 triggers were identified, though on manual inspection none could be classified as local seismic events.

- Broadband seismic arrays are typically used to detect teleseismic arrivals (large, distant earthquakes). We searched our data for teleseismic arrivals identifying 25 such events, the largest being from a magnitude 7.7 earthquake occurring in Pakistan.

- Using the earthquakes detected during hydraulic stimulation at Preese Hall, Blackpool as a template, we estimated the minimum earthquake magnitude that could be detected by our triggering algorithm. Assuming an event 2 km directly below the drilling site, we find that the smallest event that our array would have been capable of detecting using an automated picking algorithm is $M_L$ = -0.2. This is slightly below the limit of what is required by the proposed traffic light scheme.

# 1. Introduction

The operating company Cuadrilla Resources carried out exploratory drilling at the Lower Stumble site, Balcombe, West Sussex from August – September 2013. Although there were no plans to use hydraulic fracture stimulation on this exploratory well targeting an oil-bearing limestone formation at this stage, Cuadrilla have raised the possibility that such techniques could be used in the future if they feel it would improve recovery rates.

Public awareness of hydraulic fracture stimulation of oil and gas wells (colloquially shortened to "fracking") has grown in recent years, with the development of a vocal and demonstrative opposition to the technique. This opposition culminated in extensive protests around the Balcombe drilling site during operations. Although the concerns of opposition groups are multifaceted, particular local concerns at Balcombe centred on the potential impact of induced seismicity on the Ouse Valley viaduct. This railway bridge, built in 1841, still carries the London-to-Brighton main line.

In order to address these public concerns, as well as to address issues surrounding the suitability of various options for monitoring hydraulic stimulation operations in the UK, we undertook to deploy a seismic monitoring array around Cuadrilla's Balcombe drilling site for the duration of their operations.

Europe, and the UK in particular, is on the cusp of a significant increase in unconventional gas development. The BGS resource estimate for the Bowland shale alone reports over 1,300 trillion cubic feet of gas in place. However, local environmental concerns persist over the potential impacts of unconventional gas developments. It is vitally important that appropriate environmental monitoring protocols are developed at an early stage. Such monitoring should include water and air quality measurements, as well as seismic monitoring. It is on the need for seismic monitoring during shale gas development that this report focuses.

## 1.1. Hydraulic Fracturing and Induced Seismicity

Examples of felt (i.e. of sufficient magnitude to be felt by the local population) seismicity triggered by hydraulic fracturing for shale gas are rare (Davies et al., 2013). Of more than one million stimulated wells (Montgomery and Smith, 2010) in the USA, there is only one known example where stimulation has triggered felt seismicity. In January 2011, a series of 43 earthquakes were located by the Oklahoma Geological Survey in the Eola Field, with duration magnitudes ($M_D$) between $M_D = 1.0$ and $M_D = 2.8$, occurring within 24 hours of the hydraulic stimulation of a well in this field (Holland, 2011).

Outside of the USA, in 2012, the British Columbia Oil and Gas Commission reported 38 anomalous seismic events that occurred in the Horn River Basin between 2009 and 2011, with local magnitudes ($M_L$) between $M_L = 2.2$ and $M_L = 3.8$ (B.C. OGC, 2012). Owing to the remoteness of the Horn River Basin, the majority of these events were not felt by the public. These events have been attributed to extensive hydraulic stimulation in the Horn River Shale that occurred during this time.

In 2011, Cuadrilla drilled their first well targeting the Bowland Shale at Preese Hall, near Blackpool. Within 24 hours of the 2$^{nd}$ fracturing stage, an $M_L = 2.3$ event was felt by the local population. Further seismicity was felt after the 4$^{th}$ and 5$^{th}$ stages, with the largest event having $M_L = 1.5$ (de Pater and Baisch, 2011). The deployment of a local seismic monitoring array during the 4$^{th}$ and 5$^{th}$ stages, in combination with re-analysis of data from the BGS National Network allowed the identification of a total of 50 events, with magnitudes ranging from $M_L = -2.0$ to $M_L = 2.3$ (Eisner at al., 2011).

## 1.2. Traffic Light Scheme

In light of the seismic events induced at Preese Hall, the Department of Energy and Climate Change imposed a traffic light scheme to prevent the triggering of felt seismicity during hydraulic stimulation (Green et al., 2012). This scheme requires that operators do not trigger seismic events larger than $M_L = 0.0$ (green scenario). Where events with magnitude between $M_L = 0.0$ and $M_L = 0.5$ are detected, the stimulation may still be completed, but with an additional flowback period, intended to reduce pore pressures after the stimulation. If an event larger than $M_L = 0.5$ is triggered, the stimulation must be shut down immediately, with an extensive period of flowback. If no further seismicity occurs with magnitude larger than $M_L = 1.5$ during the stimulation, or $M_L = 1.0$ during flowback, then the operator has the option of re-fracturing the same stage. However, if these thresholds are exceeded, the operator must cease stimulation and move on to the next stage of the well.

The proposed traffic light scheme therefore requires that events as small as $M_L = 0.0$ be robustly identified, and their magnitude accurately characterised. This is beyond the capability of the existing BGS National Network[1], which does not typically identify events smaller than $M_L = 1.0$, meaning that dedicated seismic monitoring arrays will be required for all future hydraulic stimulation operations.

## 1.3. Our Aims

No hydraulic stimulation was planned during the current monitoring period. Given this, there was no possibility of detecting injection-induced seismic events. Nevertheless, our deployment was intended to serve a number of purposes.

- **Public Perception** – Public understanding of injection-induced seismicity issues is generally poor. There is often little appreciation for what is meant by earthquake magnitude scales – for example that most earthquakes induced by injection activities are too small to be able to cause damage to buildings or infrastructure. Drilling at Balcombe received extensive media coverage. A case example of how future hydraulic fracturing sites can be monitored using seismic methods, and in particular a demonstration of the capabilities of such instruments, will be of interest to the general public.
- **Baseline Monitoring** – The current traffic light scheme proposes that operational decisions be made based on events as small as $M_L = 0.0$. The existing BGS network is not designed to monitor earthquakes of this low magnitude. However, the Gutenberg-Richter formula as applied to the UK's earthquake catalogue implies that over 5,000 such events occur in the UK annually. In order to distinguish naturally occurring low-level seismicity from that induced by shale gas operations, baseline monitoring that characterises regional seismicity will be required prior to the start of operations.
- **Detection Threshold** – The magnitude of earthquake that can be detected is dependent on the background noise levels at the deployed seismometers. The English countryside, while typically characterised as a quiet and sleepy place, can in fact be a noisy place for seismometers. Potential sources of noise include rail lines, farm machinery, rivers, and major roads. Microseismic monitoring arrays can be deployed that are capable of monitoring events as small as magnitude -3.0. However, such arrays are expensive, requiring either the installation of geophones in boreholes, or the deployment of 1,000s of surface geophones, and typically costing over £1 million. In this deployment we aim to determine whether smaller, temporary seismic arrays, as typically deployed by academic seismologists, have sufficient detection capabilities to identify $M_L = 0.0$

[1] http://www.earthquakes.bgs.ac.uk/monitoring/detection_capability.html

earthquakes in a noise environment typical of the English countryside, as required by the traffic light scheme.

## 2. Balcombe Deployment

The Balcombe Seismic Array consisted of four stations, coded BA01 – BA04, deployed as per the map in Figure 1. Each site had a Nanometrics Trillium 120PA broadband seismometer[2] and a Nanometrics Taurus data logger[3] with external GPS, and was powered by two 65Ah batteries.

Three of the sites (BA01 – BA03) were burial installations. These involved digging a pit, laying a levelled concrete slab and then deploying the sensor on the slab (Figure 2). The sensor was then protected with an insulating cover and a waterproof, isolating cover before being buried. This ensures that the temperature of the sensor remains quite stable and the isolating cover minimizes the impact of surface noise (e.g. rain, wind). All cabling was protected in firehose and channelled into a surface-deployed Zarges case containing the data-logger and batteries.


*Figure 1: Area map of Balcombe, the seismic array (yellow pins labelled BA01 – BA04), the drill pad (red pin) and the proposed drill line (white line). Of specific interest is the railway line that snakes from the centre top of the map, to the West of Balcombe village and to the East of the drill pad, exiting the map to the East of BA04. BA04 was located close to the line to monitor train noise.*

[2] http://www.nanometrics.ca/products/trillium-120-ppa
[3] http://www.nanometrics.ca/products/taurus

The fourth station (BA04) was a surface installation inside a barn. This had the same slab and insulation as the pit deployments but was levelled on the floor of the barn with the GPS located outside on the roof.

The Trillium sensors have internal noise below or very near to the NLNM (New Low Noise Model) from 120 seconds to 100 Hz making them a true broadband sensor unlike the high frequency geophones usually used by the industry. Each station recorded 3 channels at 250 sps with continuous GPS and we had 100% data recovery for the 3-month recording period from July 1st/2nd to September 24th/25th.

All sites were subject to considerable local noise, be it cars, cows, trains, pheasants, trees, joggers, protestors or tractors. This was expected and does raise the minimum noise floor of the array but does not destroy any coherent signals passing across the network.

*Figure 2: Seismometer deployment at BA03. The green dome-shaped object is the sensor resting on an insulating base laid on the levelled paving slab at the bottom of the hole. The blue tubing is the firehose through which all cables are threaded to protect them from rodents. The grey box is the Zarges case containing the batteries and the data logger.*

## 2.1. Data Archiving

The full dataset recorded during this deployment will be made available to interested parties. The waveforms have been archived at the IRIS DMC[4] in seed format under the FDSN temporary network code Y2 (2013) and are publicly available using the standard access tools available online.

[4] http://www.iris.edu/dms/nodes/dmc/

# 3. Data Processing

The data was converted from Nanometrics store file format to SAC[5] and miniseed[6] formats using the Nanometrics Apollo Project software. A dataless seed volume was created using response information provided by Nanometrics and station information recorded during deployment. The response information allows us to plot the true ground motion at each site as well as the ground acceleration that the instruments natively record.

## 3.1. Seismogram Characteristics

The recordings at the four Balcombe stations show various characteristics. For example, station BA04 is only 150 m from the railway and therefore contains higher levels of train noise than the other stations.

There are many unidentified sources of noise such as traffic, people or animal movement and weather. However, these surface disturbances have different frequency contents and signal shapes to those expected from microseismic events or larger earthquakes. During the monitoring period we have not identified anything we consider to be a local earthquake or a microseismic event. Figure 3 shows all earthquakes identified on the BGS earthquake catalogue between 1st July 2013 and 25th September 2013. No earthquakes are reported within 200 km of the drilling site, and our automated triggering algorithm (see below) did not detect any of the earthquakes plotted in Figure 3.

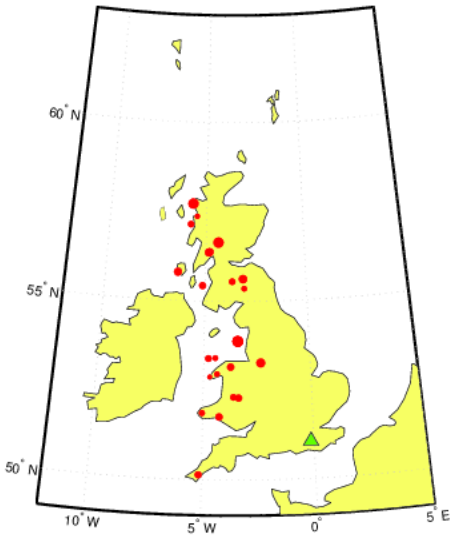


*Figure 3: Earthquakes in the BGS catalogue occurring during our monitoring period. All of the events (red circles) were greater than 200 km distance from our array (green triangle), and none were detected by the array.*

The signals from passing trains can be seen on the data recorded at all the stations, particularly clearly at BA04 which is only ~150 m from the train line. Figure 4 shows an example recording of a train at all four stations. We can establish this train was coming from the North because it is recorded at BA02 first, then BA01 and then BA04. At BA03 the train signal is difficult to distinguish from the background noise.

[5] http://www.iris.edu/files/sac-manual/
[6] http://www.iris.edu/dms/nodes/dmc/data/formats/

Using the local magnitude scale for the UK, as published by Ottemöller and Sargeant (2013), we calculate an equivalent earthquake magnitude for the train signals. $M_L$ is given by

$$M_L = log(A) + 0.95\ log(R) + 0.00183R - 1.76 \qquad [1]$$

where A is the amplitude of ground displacement in nanometres (measured on the horizontal component with traces filtered to simulate the Wood-Anderson seismograph) and R is the hypocentral distance (the distance to the location of the earthquake) in km. The maximum amplitude of the train signal at station BA04 is approximately equivalent to the ground motion that would be caused by an $M_L = 0.3$ earthquake located 150 m from the station.

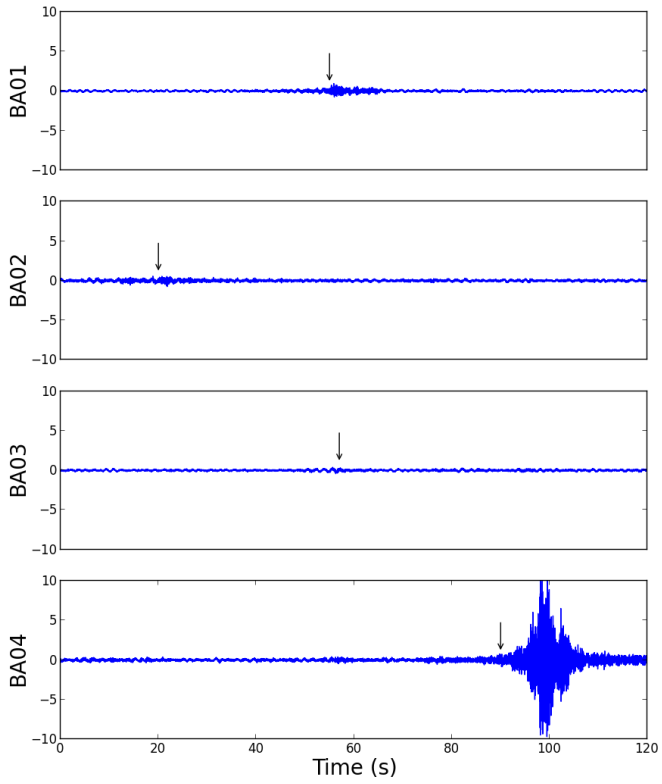


*Figure 4: Recordings at each of the sites in the network when a train is passing through Balcombe. The arrival of the wave from the train is marked by the arrows for each station. The amplitude scale on the y-axes are the same for all stations, i.e. the amplitude of the train signal at BA04 is at least 10 times larger than at the other sites.*

The drill site is approximately 1.5 km from station BA04. For an earthquake occurring at 2 km depth, the hypocentral distance to station BA04 would be 2.5 km. The ground motion at BA04 resulting from an $M_L = 1.5$ earthquake (the same magnitude as the 27 May 2011 Preese Hall earthquake) at this hypocentral distance would be similar to that produced by the passing trains.

Figure 5 superimposes the modelled response of a typical $M_L = 1.5$ earthquake recorded at a hypocentral distance of 3 km on to an example of the passing train at station BA04. Although the amplitude of the train and earthquake signals in Figure 5a is similar a trained analyst is able to see a difference in characteristic between the signals. In addition the signals can be distinguished because the frequency content of the signals (shown by the spectrogram in Figure 5b) is different: the train signal has significant low frequency component in the first part of the

signal and higher frequencies when the train is closest to the station. However, since the amplitudes of the earthquake and train signals are similar in Figure 5a the earthquake may not be detected at this station if a train was passing at the same time.

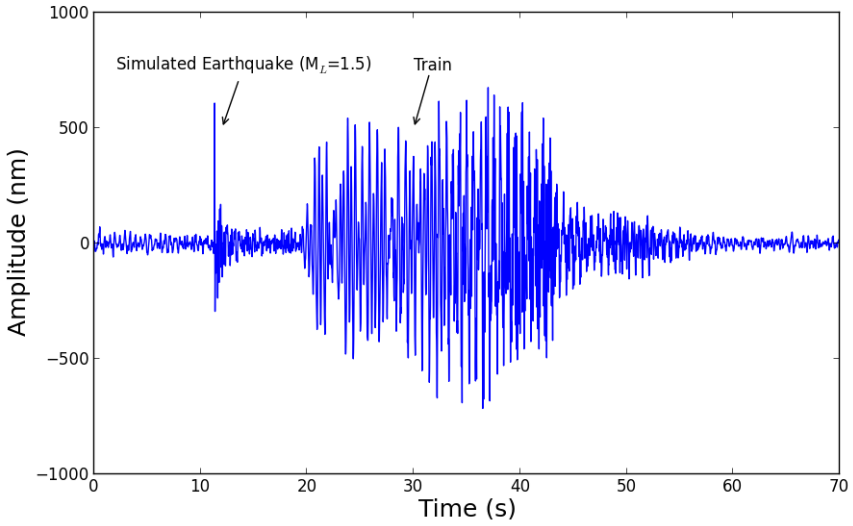


*(a)*

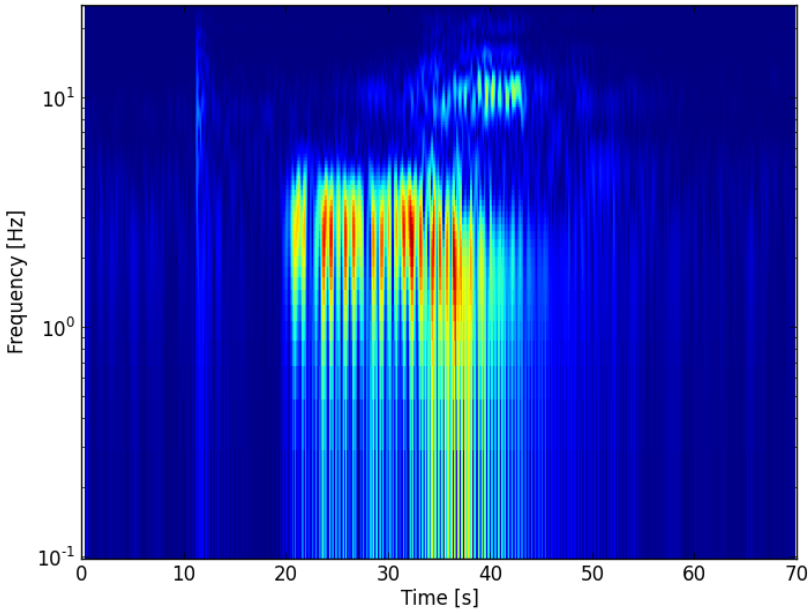


*(b)*

*Figure 5: a) A recording of a passing train at BA04 compared to recording of earthquakes that could be expected for a simulated event at 3 km with magnitudes $M_L$ = 1.5; b) A spectrogram of a). This gives the frequency content of the seismogram with bright colours (yellow, green, red) indicating larger amplitudes at that frequency and blue colours indicating small amplitudes at that frequency.*

### 3.2. Drilling Activities

The seismometers recorded drilling noise from drilling at the Balcombe test well. This is observed as increased constant noise levels, particularly at station BA01, which is closest to the drill site. Figure 6 shows recordings from station BA01 before and during drilling. The

amplitude of the background noise at BA01 approximately doubles during drilling activities. As shown in the spectrogram in Figure 5b above, different sources have different frequency contents. Figure 7 illustrates the noise levels (in dB) at site BA01 before (early July) and during (early August) drilling at Balcombe. The spectra show increased noise levels between periods of 1 s and 10 s while drilling is taking place in August.

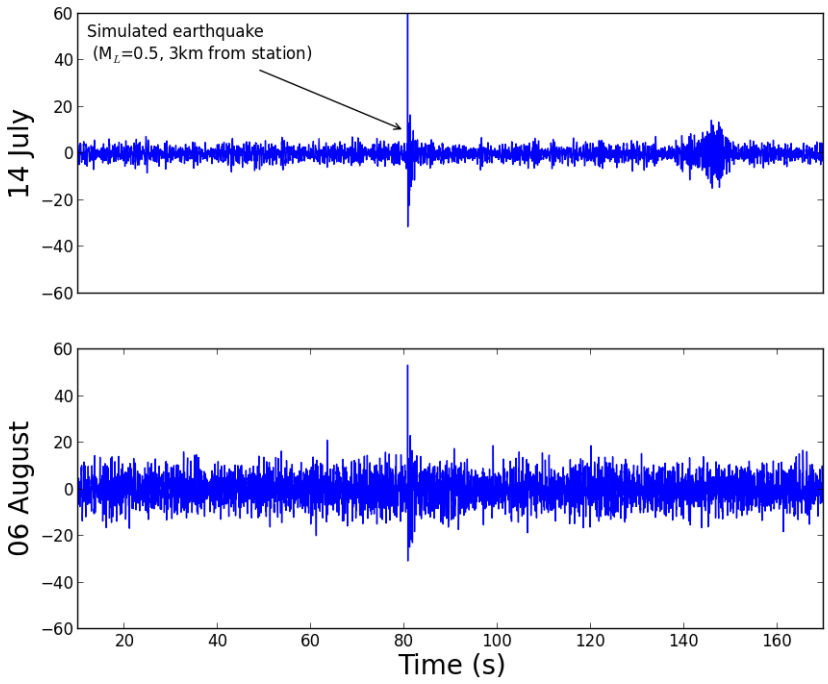


*Figure 6: Example of seismograms at BA01 before (14th July) and during (6th August) drilling at the Balcombe test site. An example waveform for a simulated $M_L$ = 0.5 earthquake at 3 km is added. The background noise increases during drilling but the earthquake arrival remains obvious.*

An example recording of a $M_L$ = 0.5 earthquake at 3 km from the station is superimposed on Figure 6. The earthquake arrival is obvious in both seismograms and the drilling noise would not pose a problem for event detection (described in more detail below).

# 4. Results

## 4.1. Triggers

An automated triggering algorithm was used to identify potential triggers for further study. The triggering algorithm was based on that described by Allen (1982), as is commonly used by the BGS (Baptie, pers. comm.). A characteristic function (CF) is defined as

$$CF(i) = Y(i)^2 + 3(Y(i) - Y(i-1))^2$$

where *Y(i)* is the seismogram value at time sample *i*, *Y(i-1)* is the seismogram value at the previous time sample, and *CF(i)* is the resulting characteristic function.

The raw seismograms are sampled at 250 Hz. To speed computation time, the data are resampled to 100 Hz, followed by bandpass filtering with corner frequencies of 2 Hz and 45 Hz. Short (5 samples, or 0.05 seconds) and long (200 samples or 2 seconds) term averages of the *CF* are taken

over both the North and East horizontal components of Stations BA01, BA02, and BA03. BA04 is not used in the triggering analysis, due to the increased noise of passing trains. A threshold of STA/LTA $\geq 7.5$ is used to define a potential trigger. This threshold must be exceeded on at least one of the two horizontal components of each station within a 2 second window. When a potential event has been declared, the traces from all 4 stations are stored for manual analysis.

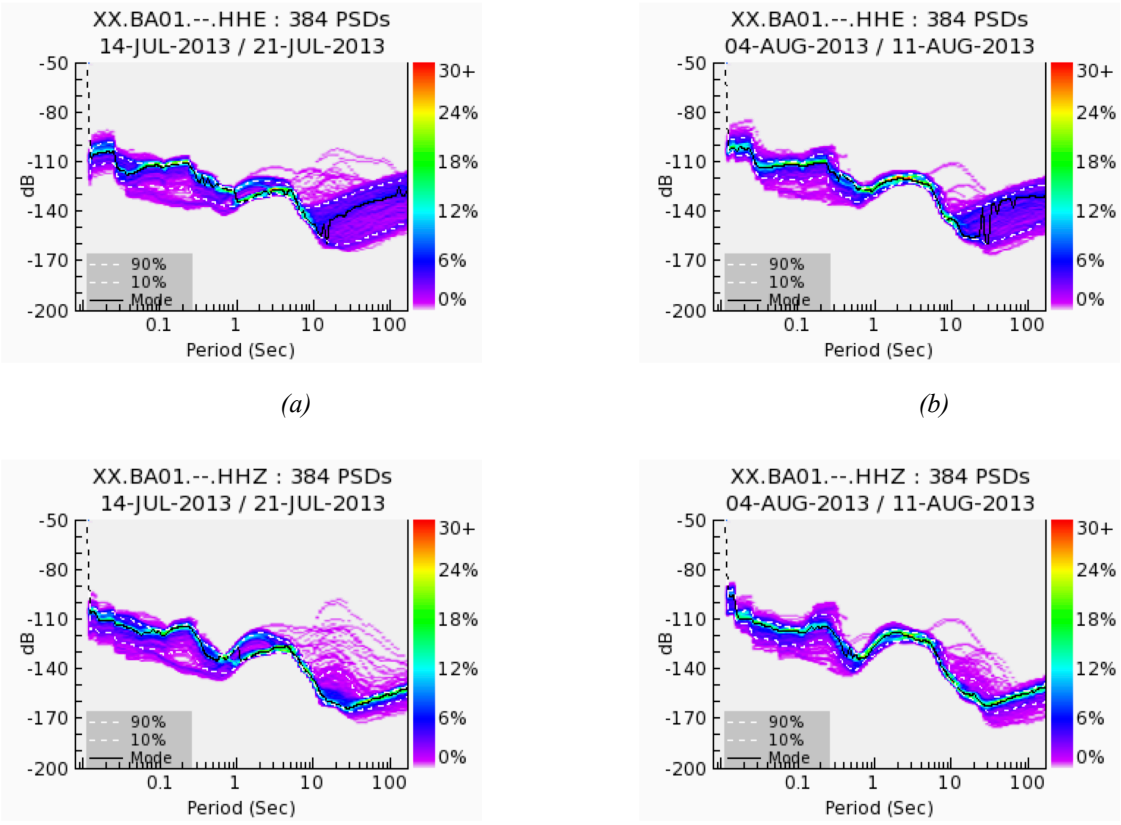


*Figure 7: Power spectral density plots for data recorded at BA01 a) and c) before (July) and b) and d) during (August) drilling. The amplitude at each wave period is given in dB. Plots for a) and b) horizontal and c) and d) vertical components are shown.*

A total of 134 potential triggers were identified in this manner. These potential triggers were processed manually to determine whether the trigger represents a local earthquake or is a mistaken trigger induced by the coincidence of increased noise at each station. Manual inspection did not reveal any waveforms with the characteristics of a local earthquake.

An example from 6$^{th}$ July of the type of arrival detected by the triggering algorithm is given in Figure 8. This does not look like an earthquake because it seems to be part of a short sequence of repeating noise events seen at BA01, BA02 and BA03. Usually when an earthquake occurs P and S waves are observed with different amplitudes on the horizontal and vertical components and this is not the case in Figure 8. BA04 is shown for completeness but is not included in the triggering algorithm due to the noise from the trains and at this time it shows similar noise events to the other stations.

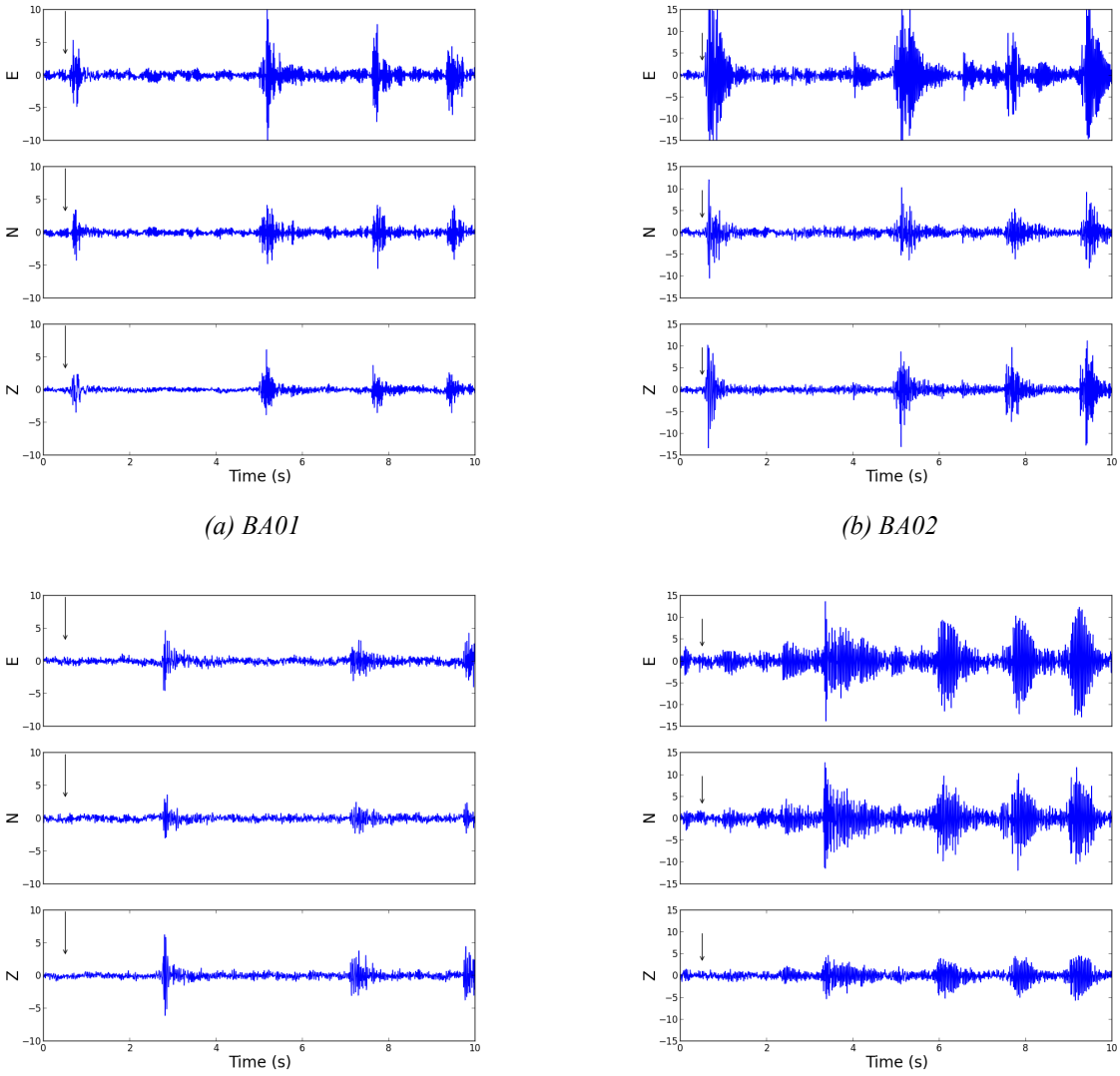


*(a) BA01* *(b) BA02*

*(c) BA03* *(d) BA04*

*Figure 8: Seismograms recorded at all four stations around the time a detection was reported by the triggering algorithm. The black arrows show the trigger time. The horizontal (E and N) and vertical (Z) components are shown.*

## 4.2. Teleseismic Arrivals

Broadband seismometers are often used to detect larger earthquakes from around the world. Large earthquakes from the other side of the planet produce enough energy to be detected. We therefore examined our seismograms for so-called teleseismic arrivals as well. Unlike local earthquakes, seismic waves arriving from distant earthquakes will have similar waveforms at each of the four stations. As such, teleseismic arrivals can be identified by searching for similarities between waveforms on different stations. This is done via a cross-correlation analysis. The vertical component of each station is windowed at 10-minute intervals, and cross-correlated with the vertical component of each other station. A potential teleseismic trigger is declared where the mean cross-correlation value of two aligned traces (within 2 seconds) is 50 times greater than the cross-correlation value of non-aligned traces (greater than 2 seconds). A potential teleseismic event is declared where this threshold is exceeded for 3 of the 6 cross-correlated trace pairs.

A total of 32 potential teleseismic triggers were identified using the cross-correlation triggering algorithm described above. The arrival times of these triggers were compared with global earthquake catalogues (the USGS National Earthquake Information Center[7]). Expected arrival times for these events were computed using a 1D Earth velocity model by employing the TauP seismic travel time calculator[8]. For 25 of the 32 potential triggers, modelled arrival times matched with the triggered interval, implying that a teleseismic arrival had been observed. Figure 9 shows examples of teleseismic arrivals. Figure 10 maps all the teleseismic earthquakes detected, which are listed in Appendix 2.

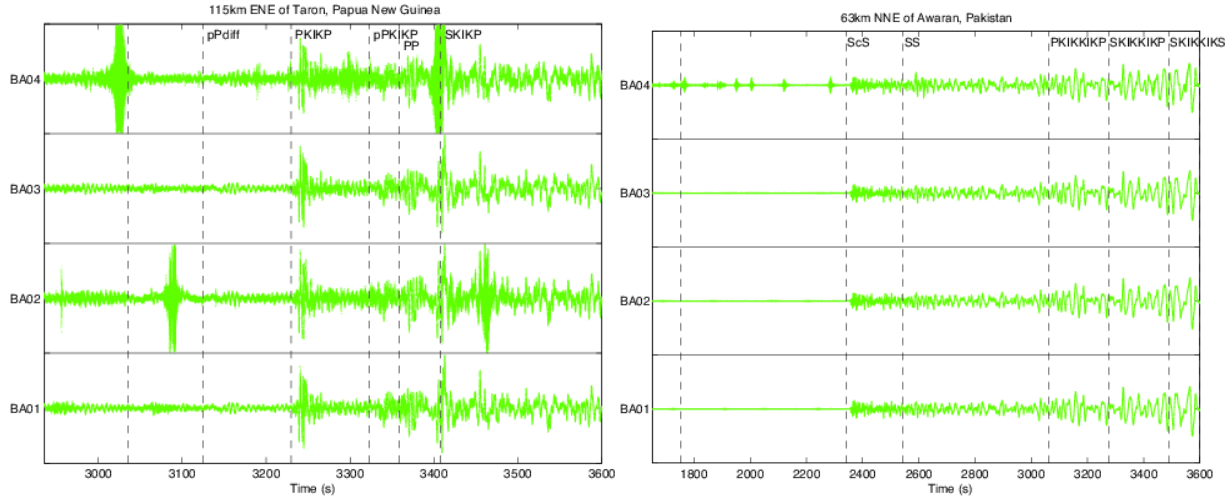


*Figure 9: Example teleseismic arrival, showing vertical components from all 4 stations. Magnitude 7.3 earthquake occurring near Taron, Papua New Guinea at 18:35 (UTC) on the 7th July, and magnitude 7.7 earthquake occurring near Awaran, Pakistan, at 11:19 on the 24th September. Arrival times predicted from a 1D Earth velocity model are marked for different phases.*

### 4.3. Detection Threshold

In the absence of any detected local earthquakes, we sought to determine the minimum magnitude event that could be detected using our array, given the recorded noise levels. Without recorded local events with which to calibrate detection thresholds in the manner described by Gaucher (2013), our computed detection thresholds should be considered to be approximate values only.

We use the local magnitude relationship described by Ottemöller and Sargeant (2013), outlined above, as a proxy for the expected event magnitudes. We also use the event waveforms recorded during hydraulic fracturing at Preese Hall, as they represent a good example of a small magnitude triggered event recorded on a local monitoring array. Specifically we use the waveforms recorded at local station HHF during the $M_L = 1.5$ earthquake on May 27th, 2011 (Eisner et al., 2011).

For a given magnitude event, we scale the Preese Hall waveforms such that their amplitudes correspond to the expected amplitude using the local magnitude scale. In order to determine hypocentral distances, we assume that our modelled event occurs directly below the Balcombe drill site, at a depth of 2 km. To determine whether an event of given magnitude could have been detected, we superimpose our modelled earthquake waveforms onto the recorded traces from our four stations. Our composite waveforms are then subjected to the same processing flow and

[7] http://earthquake.usgs.gov/earthquakes/search/
[8] http://www.seis.sc.edu/taup/

triggering algorithm described above, establishing whether the event would have been identified above the noise levels.

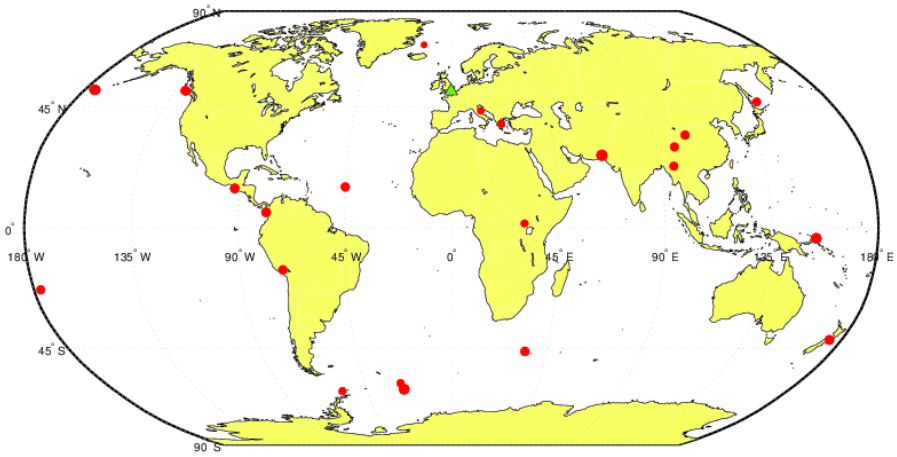


*Figure 10: Locations of earthquakes (red circles) with teleseismic arrivals detected on the Balcombe seismic array (green triangle) (events are listed in Appendix 2).*

We repeat this process, using traces recorded before and during drilling in order to determine whether the increased drilling noise would affect event detection. Figure 11 shows examples of our composite waveforms, including a simulated $M_L = 0.5$ event, from both before (Figure 11a) and during (Figure 11b) drilling. We find that our automated triggering algorithm is capable of robustly identifying events down to $M_L = -0.2$ – $M_L = -0.4$ (depending on the noise level of the particular recorded traces used). Figure 12 shows examples of a simulated $M_L = -0.2$ event superimposed on pre- and during drilling recorded traces. We do not see any systematic difference in event detection threshold between pre- and during drilling traces. In fact, the detection limit is mainly controlled by the levels of noise on station BA02, which is further from the drilling site, and therefore has a weaker earthquake signal. The noise levels on BA02 are not substantially different during drilling.

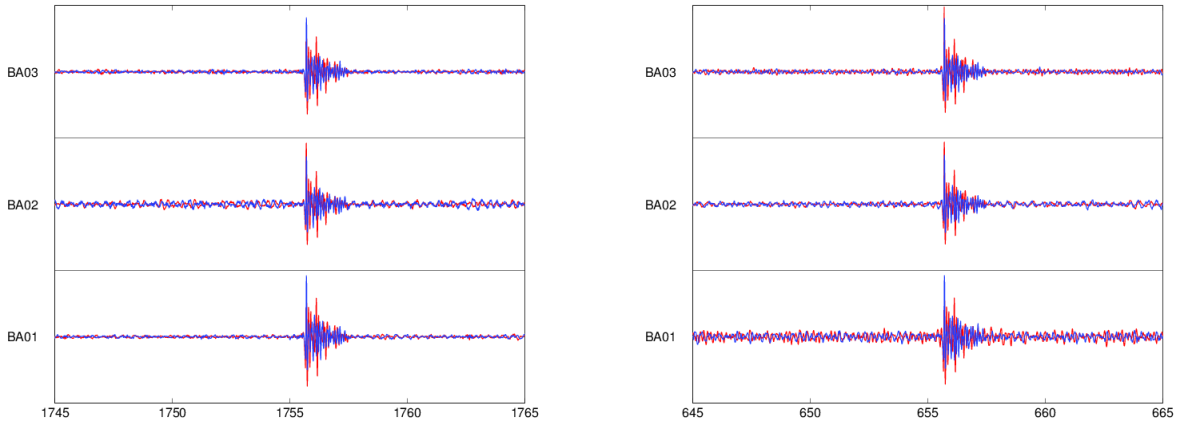


*(a)* *(b)*

*Figure 11: Traces with a simulated $M_L = 0.5$ event superimposed on pre-drilling (a) and during drilling (b) traces. This event is easily identified by the automated triggering algorithm for both cases, despite the increase in drilling noise on BA01.*

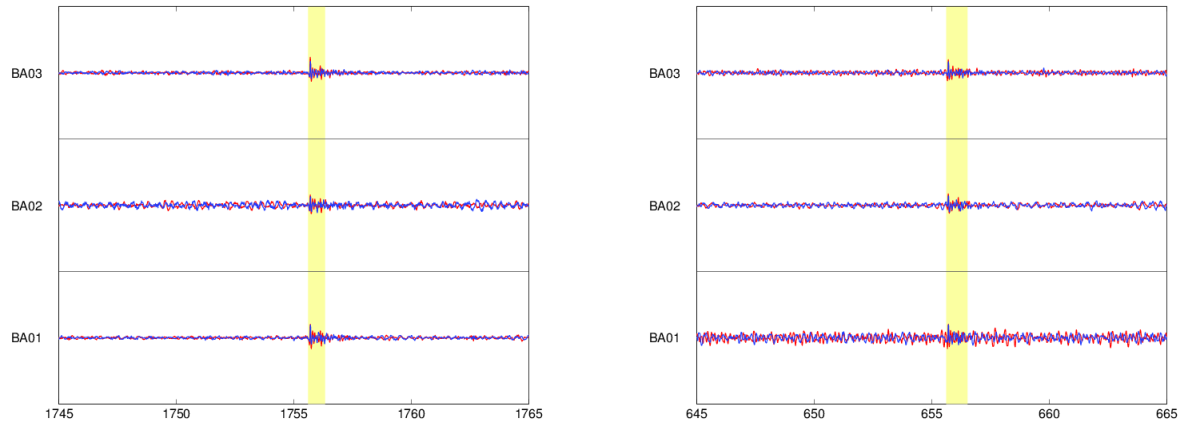


*(a)* *(b)*

*Figure 12: Traces with a simulated $M_L$ = -0.2 event superimposed on pre-drilling (a) and during drilling (b) traces. The event is highlighted with yellow to aid identification. This event is at the limit of detectability using the automated triggering algorithm.*

The limiting factor in the triggering is the distance of BA02 from the assumed simulated hypocentre 2 km below the drilling site. This hypocentre is 2.5 km from station BA02 with an epicentral distance of 1.45 km. According to Equation 1, an $M_L$ = -0.2 produces a recorded amplitude of 15 nm at a hypocentral distance of 2.5 km. Continuing to assume an event at 2 km depth and assuming a signal amplitude of 15 nm is the limit of detection, the maximum epicentral distance for a detected $M_L$ = 0.0 event would be 2.8 km. The estimated detection area covered by the array for $M_L$ = -0.2 and $M_L$ = 0.0 earthquakes at 2 km deep is illustrated in Figure 13.

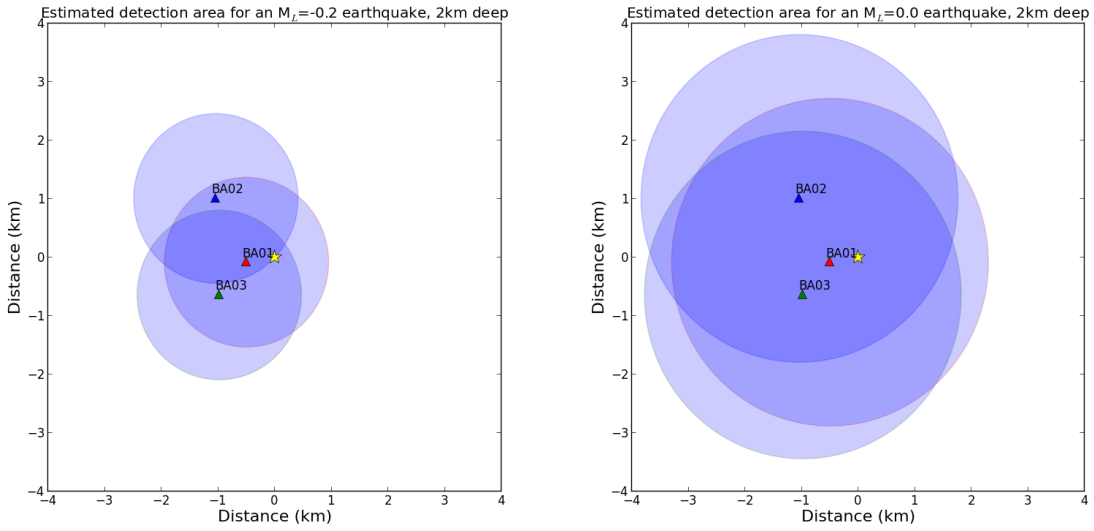


*(a)* *(b)*

*Figure 13: The estimated detection areas for BA01, BA02 and BA03 assuming an event at 2 km depth for (a) $M_L$ = -0.2 and (b) $M_L$ = 0.0. The overlap of the 3 circles in (a) and (b) illustrates the estimated coverage of the array if a trigger on all 3 stations is required. The yellow star is the location of the drill pad.*

## 5. Discussion and Recommendations

This report summarises a 3-month seismic monitoring project at the Cuadrilla Resources drilling site near Balcombe in West Sussex, England. The monitoring has not revealed any local seismicity, either naturally occurring or induced by the drilling operation. However, the project does highlight a number of important issues with environmental impact monitoring in sites of hydraulic fracture stimulation (fracking) and sub-surface waste storage (e.g., CCS). Here we discuss the implications for operators and regulators, making recommendations for future monitoring.

Sparse surface arrays of seismometers are ideally suited to environmental monitoring of induced seismicity. Such networks can be deployed at a fraction of the cost of commercial arrays typically used to monitor the efficacy of hydraulic stimulation (e.g., downhole monitoring or dense surface or shallow-borehole arrays).

Any anthropogenic activity such as hydraulic stimulation requires good baseline monitoring before activities start. This is beneficial for operators, as it reveals background levels of seismic activity and the location of potentially problematic active faults that can be avoided in hydraulic fracturing operations. It is also important for regulators to have a good understanding of the nature of local seismicity, especially with contentious issues regarding induced versus naturally occurring seismicity.

The project has highlighted the importance of good site selection for seismometers and other monitoring equipment. It is important to avoid cultural noise where possible. For example, trains crossing a local railway bridge generate ground motion at our BA04 sensor equivalent to an $M_L = 1.5$ event at a hypocentral distance of 3 km. In general, these issues can be addressed through advance permitting and good lines of communication with local landowners. We also recommend that array design studies be conducted in order to optimise detection thresholds and to assess data coverage.

A real-time system is needed for monitoring. The University of Bristol Geophysics Group is currently exploring methods of using mobile phone technology to communicate with sensors in near-real-time. The rapid analysis of sparse array data can be used to detect seismic events down to the magnitudes required by a traffic light system (e.g., $\geq M_L = -0.2$).

The project raises the issue of whether or not the recently proposed UK traffic light system for monitoring hydraulic stimulation is fit for purpose. Under the current 'traffic-light' system, operational decisions will be taken based on events with $M_L = 0.0 - 0.5$. Accurate and independent estimates of induced event magnitudes are therefore required. To do so robustly is a challenging task for events of such low magnitudes. The current work demonstrates that the ground motion associated with train vibrations can easily generate significant ground motion that exceeds the 'traffic light' threshold.

Equally, current UK seismic catalogues do not commonly contain information about events as small as magnitude 0 (typically, the UK catalogue is complete to $M_L = 2.0$). Applying the Gutenberg-Richter relationship to known rates of seismicity in the UK implies that there are over 5,000 undetected events naturally occurring each year that would trigger an 'amber warning', and over 2,000 that would trigger a 'red light' and stop any local shale gas operation. As noted, sparse seismic networks – on the order of 20-50 seismometers – can be used to monitor induced seismicity in shale gas regions. Baseline surveys of seismicity that are complete down to the low

'traffic light' magnitudes will be needed if we are to unambiguously discriminate between naturally occurring and triggered seismic events.

It will also be necessary to produce reliable and accurate magnitude estimates. Such estimates are well known to vary widely depending on the methods used to calculate event magnitude. Local magnitudes ($M_L$) are relatively simple to calculate but are not derived from any physical aspect of the earthquake source. Moment magnitude, $M_W$, provides a direct measurement of magnitude linked to the seismic moment released by the earthquake, which in turn is determined by the size of the earthquake rupture, and the amount of slip. In addition, $M_W$ provides the only method for accurate comparison of magnitude between regions. This is because it does not depend on the applicability of an empirically derived relationship to that particular area.

Given the direct link between $M_W$ and the physical parameters of an earthquake, we suggest that $M_W$, rather than $M_L$, is a more appropriate measure of magnitude to be used in a traffic light scheme. Figure 13, taken from Ottemöller and Sargeant (2013), compares estimated local and moment magnitudes for a selection of UK earthquakes. We note that the difference between $M_L$ and $M_W$ can be as high as 0.5 magnitude units and for smaller events $M_L$ is expected to underestimate $M_w$ by up to 1.0 units (Deichmann, 2006).

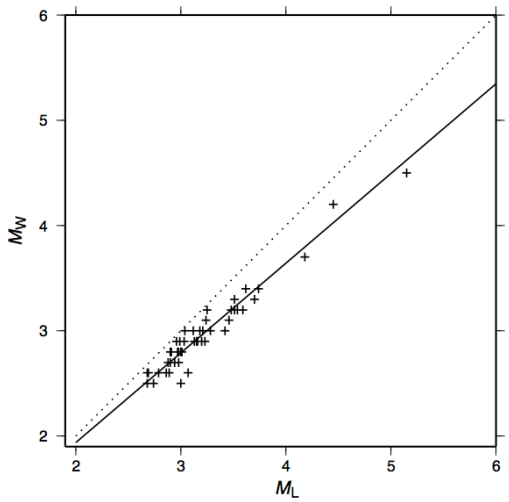


*Figure 13: Comparison of $M_L$ and $M_W$ made by Ottemöller and Sargeant (2013) for a selection of UK earthquakes. The dashed line gives $M_W = M_L$. The differences between $M_L$ and $M_W$ can be significant – as much as 0.5 magnitude units.*

Furthermore, like any measurement of a natural system, all magnitude estimations, whether $M_L$ or $M_W$, will have an uncertainty or error associated with the measurement. For larger magnitude events, signal-to-noise ratios (SNR) are large, and so this uncertainty is typically small, and therefore errors are rarely reported. However, for small-magnitude events, this uncertainty, and therefore the errors associated with any measurement, can be larger. It is not currently clear how this uncertainty should be incorporated into the traffic light scheme as it currently stands.

The University of Bristol Geophysics Group has recently developed a series of recommendations for accurate estimates of $M_W$, mitigating against sources of uncertainty that can lead to error bars of almost an order of magnitude (Stork et al., 2014). These are:

- Use focal mechanism solutions to compute source radiation pattern corrections.
- If SNR is low use S-waves only.
- Use recordings where SNR > 3.0.
- Use recording frequencies >1000 Hz if fitting model spectra to amplitude spectra where $M_W < 0$.

- Use individually estimated time windows to compute the amplitude spectra. If this is not possible due to data volume, check window length is appropriate for a subset of typical events.
- Understand the limitations imposed by the velocity model or event location errors.
- Use at least 4 receivers to make magnitude estimates.
- If attenuation (Q) is known, correct recordings for attenuation and measure the spectral level at low frequencies.

A pool of seismometers can be quickly deployed in regions of shale gas development. A sparse network can be used to monitor and locate events of significant magnitude in semi-real-time. Furthermore, such a network would provide an independent estimate of event magnitude, information that is needed for 'traffic-light' monitoring of induced seismicity. It is important for regulatory purposes and public confidence that such a seismic network is established and operated by institutions independent from the oil and gas operators. The British Geological Survey and allied UK Universities have the experience and necessary expertise to deploy and operate such a seismic network.

A small research and development investment at this stage would address a number of concerns, both for regulators and operators, but would also help establish public confidence in the management of such operations. Important questions that need to be addressed include:

- What is the baseline rate at which low-magnitude ($M_L = 0 – 2$) events occur naturally in an area?
- What monitoring period is required to provide a meaningful baseline?
- What is the minimum size of an array that can be deployed for environmental impact monitoring (considerations include detection, event magnitude estimation, resolution)?
- What is the optimal array configuration (distributed versus clusters)?
- What is the best seismic sensor for such monitoring (broad-band versus short period; single component versus three component)?
- What is the best approach for real-time seismic monitoring?
- What is the most effective means of noise suppression in areas of high cultural noise?

## 6. Acknowledgements

We would like to thank the Balcombe Estate for allowing us to access their land and to deploy seismometers on it. The seismometers we used were provided by the CoMITAC Project[9], which receives funding from the European Research Council under the European Union's 7th Framework Programme (FP7/2007-2013)/ERC Grant agreement no. 240473 "CoMITAC". Future research in this area will be funded by NERC Grant NE/L008351/1: Microseismic Impact Assessment for Shale Gas Stimulation (MIA). We also thank Philip Usher and Mary Maller for their assistance in deploying and servicing the seismometers, and Brian Baptie and Peter Styles provided the waveforms from the Preese Hall earthquakes.

## 7. References

Allen, R. 1982. Automatic phase pickers: their present use and future prospects: Bulletin of the Seismological Society of America 72, S225-S242.

B.C. Oil and Gas Commission 2012. Investigation of observed seismicity in the Horn River Basin: Report by the BCOGC.

Davies, R., Foulger, G., Bindley, A., Styles, P. 2013. Induced seismicity and hydraulic fracturing for the recovery of hydrocarbons: Marine and Petroleum Geology 45, 171-185.

de Pater, C.J. and Baisch, S. 2011. Geomechanical study of Bowland shale seismicity: Report published by Cuadrilla.

Deichmann, N. 2006. Local magnitude, a moment revisited, Bulletin of the Seismological Society of America, 96, 1267–1277.

Eisner, L., Janská, E., Opršal, I., Matoušek, P. 2011. Seismic analysis of the events in the vicinity of the Preese Hall well: Report published by Seismik S.R.O..

Gaucher, E. 2013. Effective detection capability of a local seismic network: 2nd EAGE Sustainable Earth Sciences Conference, Expanded Abstracts, A022.

Green, C.A., Styles, P., Baptie, B.J. 2012. Preese Hall shale gas fracturing review and recommendations for induced seismic mitigation: Report published by DECC.

Holland, A. 2011. Examination of possibly induced seismicity from hydraulic fracturing in the Eola Field, Garvin County, Oklahoma: Oklahoma Geological Survey Open File Report OF1-2011.

Montgomery, C.T. and Smith, M.B. 2010. Hydraulic fracturing: History of an enduring technology: Journal of Petroleum Technology 62, 26-41.

Ottemöller, L. and Sargeant, S. 2013. A local magnitude scale $M_L$ for the United Kingdom: Bulletin of the Seismological Society of America 103, 2884-2893.

Stork, A.L., Verdon, J.P., Kendall, J-M. 2014. Assessing the effect of microseismic processing methods on seismic moment and magnitude calculations: Geophysical Prospecting, *sub judice*.

[9] http://www1.gly.bris.ac.uk/CoMITAC/

## Appendix 1: Station locations

| Code | Location | Lat | Long |
|---|---|---|---|
| BA01 | Pilstye Woods | 51.047 | -0.139 |
| BA02 | Westup Farm | 51.057 | -0.147 |
| BA03 | Spicers Farm | 51.042 | -0.147 |
| BA04 | Ryelands Farm | 51.037 | -0.118 |

## Appendix 2: Teleseismic events identified during monitoring period

| Location | Date | Time (UTC) | Lat | Long | Depth (km) | Mag |
|---|---|---|---|---|---|---|
| 46km W of Kigorobya, Uganda | 02/07/2013 | 13:33:17 | 1.60 | 30.88 | 10 | 5.2 |
| 71km N of Bristol Island, South Sandwich Islands | 03/07/2013 | 20:16:39 | -58.4 | -26.371 | 140.7 | 5.3 |
| 115km ENE of Taron, Papua New Guinea | 07/07/2013 | 18:35:30 | -3.92 | 153.92 | 386.25 | 7.3 |
| 231km E of Ittoqqortoormiit, Greenland | 15/07/2013 | 11:34:26 | 70.02 | -15.98 | 10 | 4.5 |
| 218km SSE of Bristol Island, South Sandwich Islands | 15/07/2013 | 14:03:43 | -60.86 | -25.14 | 30.98 | 7.3 |
| 18km W of Chivay, Peru | 17/07/2013 | 02:37:42 | -15.63 | -71.77 | 6.59 | 6 |
| Numana, Italy | 21/07/2013 | 01:32:25 | 43.51 | 13.75 | 9.65 | 4.9 |
| 46km ESE of Blenheim, New Zealand | 21/07/2013 | 05:09:31 | -41.71 | 174.44 | 14 | 6.5 |
| 13km E of Chabu, China | 21/07/2013 | 23:45:56 | 34.49 | 104.24 | 9.84 | 5.9 |
| South Shetland Islands | 22/07/2013 | 00:05:05 | -61.60 | -58.30 | 15.95 | 5.2 |
| 244km WNW of Marion Island, Prince Edward Islands | 22/07/2013 | 07:01:42 | -46.04 | 34.82 | 10 | 6.1 |
| 288km SW of Vaini, Tonga | 24/07/2013 | 03:32:35 | -23.05 | -177.15 | 166.89 | 5.9 |
| 196km ESE of Dolinsk, Russia | 04/08/2013 | 15:56:34 | 46.94 | 145.32 | 367.35 | 5.8 |
| 6km SW of Kainouryion, Greece | 07/08/2013 | 09:06:54 | 38.75 | 22.66 | 15.6 | 5.1 |
| 7km N of Elatia, Greece | 09/08/2013 | 11:49:24 | 38.70 | 22.75 | 10 | 5 |
| 43km N of Wangda, China | 11/08/2013 | 21:23:43 | 30.07 | 97.92 | 19.66 | 5.7 |
| 98km WSW of Mutis, Colombia | 13/08/2013 | 15:43:15 | 5.78 | -78.17 | 12 | 6.6 |
| 94km ESE of Adak, Alaska | 30/08/2013 | 16:25:02 | 51.60 | -175.36 | 33.53 | 7 |
| 191km WSW of Bella Bella, Canada | 03/09/2013 | 20:19:06 | 51.22 | -130.44 | 5.5 | 6 |
| 163km SW of Bella Bella, Canada | 04/09/2013 | 00:23:12 | 51.19 | -129.90 | 9.94 | 5.9 |
| 77km SSW of Atka, Alaska | 04/09/2013 | 02:32:33 | 51.59 | -174.75 | 39.87 | 6.5 |
| Northern Mid-Atlantic Ridge | 05/09/2013 | 04:01:35 | 15.20 | -45.16 | 10 | 6 |
| 5km ESE of Ciudad Tecun Uman, Guatemala | 07/09/2013 | 00:13:29 | 14.64 | -92.10 | 67 | 6.6 |
| 48km NNE of Shwebo, Burma | 20/09/2013 | 12:24:46 | 22.93 | 95.96 | 4 | 5.7 |
| 63km NNE of Awaran, Pakistan | 24/09/2013 | 11:19:47 | 26.97 | 65.52 | 15 | 7.7 |


Bristol University Geophysics Group

School of Earth Sciences

University of Bristol

BS8 1RJ, UK

Website: www1.gly.bris.ac.uk/geophysics/

Email: gljmk@bristol.ac.uk